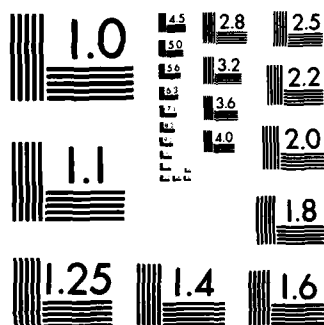END

FILM

DTIC
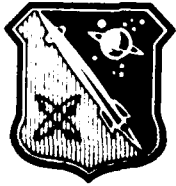
MICROCOPY RESOLUTION TEST CHART

NATIONAL BUREAU OF STANDARDS-1963-A

AD-A155 344

Final Report
for the period
1 June 1980 to
15 August 1980

Modeling the Exhaust of the Pulsed Plasma Thruster

February 1985

Author:
D. W. Yannitell

Louisiana State University
Department of Mechanical Engineering
Baton Rouge, Louisiana 70803

F049620-79-C-0038

Approved for Public Release

DTIC
ELECTE
JUN 2 3 1985
S
E
D

prepared for the: **Air Force
Rocket Propulsion
Laboratory**

Air Force Space Technology Center
Space Division, Air Force Systems Command
Edwards Air Force Base,
California 93523-5000

DTIC FILE COPY

85 06 10 101
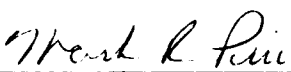
NOTICE
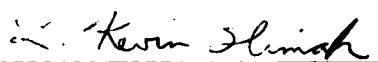
FOREWORD
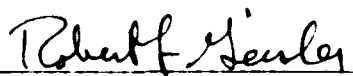
This report, Modeling the Exhaust of the Pulsed Plasma Thruster, was prepared by Daniel W. Yannitell, Associate Professor of Mechanical Engineering at Louisiana State University, while on temporary assignment to the Air Force Rocket Propulsion Laboratory. The project manager for the Air Force Rocket Propulsion Laboratory was Lt Mark Price.

This technical report has been reviewed and is approved for publication and distribution in accordance with the distribution statement on the cover and on the DD Form 1473.

MARK R. PRICE, 2Lt, USAF
Project Manager

L. KEVIN SLIMAK
Chief, Interdisciplinary Space
Technology Branch

FOR THE DIRECTOR

ROBERT L. GEISLER
Deputy Chief, Propulsion Analysis Division

REPORT DOCUMENTATION PAGE

1a. REPORT SECURITY CLASSIFICATION UNCLASSIFIED		1b. RESTRICTIVE MARKINGS			
2a. SECURITY CLASSIFICATION AUTHORITY		3. DISTRIBUTION/AVAILABILITY OF REPORT Public Release. Distribution Unlimited.			
2b. DECLASSIFICATION/DOWNGRADING SCHEDULE					
4. PERFORMING ORGANIZATION REPORT NUMBER(S)		5. MONITORING ORGANIZATION REPORT NUMBER(S) AFRPL-TR-85-005			
6a. NAME OF PERFORMING ORGANIZATION Louisiana State University	6b. OFFICE SYMBOL (If applicable)	7a. NAME OF MONITORING ORGANIZATION Air Force Rocket Propulsion Laboratory			
6c. ADDRESS (City, State and ZIP Code) Department of Mechanical Engineering Baton Rouge, LA 70803		7b. ADDRESS (City, State and ZIP Code) AFRPL/DYSO, Stop 24 Edwards Air Force Base, CA 93523-5000			
8a. NAME OF FUNDING/SPONSORING ORGANIZATION Air Force Office of Scientific Research	8b. OFFICE SYMBOL (If applicable)	9. PROCUREMENT INSTRUMENT IDENTIFICATION NUMBER F49620-79-C-0038			
8c. ADDRESS (City, State and ZIP Code) Air Force Office of Scientific Research Bolling Air Force Base, Washington, D.C. 20332		10. SOURCE OF FUNDING NOS.			
		PROGRAM ELEMENT NO.	PROJECT NO.	TASK NO.	WORK UNIT NO
11. TITLE (Include Security Classification) MODELING THE EXHAUST OF THE PULSED PLASMA THRUSTER (U)		62302F	3058	12	TB
12. PERSONAL AUTHOR(S) Daniel W. Yannitell					
13a. TYPE OF REPORT Final	13b. TIME COVERED FROM 80/6/1 TO 80/8/15	14. DATE OF REPORT (Yr., Mo., Day) 85/02		15. PAGE COUNT 34	
16. SUPPLEMENTARY NOTATION					

17	COSATI CODES		18. SUBJECT TERMS (Continue on reverse if necessary and identify by block number)
FIELD	GROUP	SUB. GR.	Pulsed Plasma, Plume Modeling, Teflon Pulsed Plasma.
21	03		

19. ABSTRACT (Continue on reverse if necessary and identify by block number)

The work presented in this report is an investigation of the plasma flow in a Teflon Pulsed Plasma Thruster (PPT), and the resulting plume. The long range goal is a theoretical model of the flow, both between and beyond the thruster electrodes, that could aid in the improvement of performance, and also predict the contamination potential of the device.

The overall model required consists of an internal portion interfaced with an external portion at the exit plane of the electrodes. Most of this report deals with the internal portion of the model. Specifically, the physics of the discharge and plasma acceleration between the electrodes are discussed, and a mathematical model is developed which appears to be consistant with the available experimental data. The investigation shows the necessity of certain additional information without which the model cannot be properly exercised. The validity of certain assumptions of magnetohydrodynamic theory is demonstrated for the nontypical plasma produced by the PPT, and logical consequences of the assumptions are...

20. DISTRIBUTION/AVAILABILITY OF ABSTRACT	21. ABSTRACT SECURITY CLASSIFICATION	
UNCLASSIFIED/UNLIMITED ☒ SAME AS RPT ☐ DTIC USERS ☐	UNCLASSIFIED	
22a. NAME OF RESPONSIBLE INDIVIDUAL Mark R. Price, 2Lt, USAF	22b. TELEPHONE NUMBER (Include Area Code) (805) 277-5240	22c. OFFICE SYMBOL DYSO

DD FORM 1473, 83 APR EDITION OF 1 JAN 73 IS OBSOLETE.

SECURITY CLASSIFICATION OF THIS PAGE

Block 19 (Continued): considered vis a vis recently obtained electromagnetic data.

A major difficulty in the modeling of the internal flow is the selection of the proper boundary conditions to be applied to the solution domain. These include conditions at the electrodes, the insulator, the ablating Teflon surfaces, and the interface with the vacuum ahead of, and behind, the plasma blobs.

Discussion of the possibilities for a model of the external, or plume, flow is less specific than that for the internal model, but the physical phenomena are discussed in light of available data, and some recommendations are made.

The principal conclusions of the research are that an internal model based on rather typical equations should be valid, but that additional experimental data are required to complete such a model, and that the boundary conditions used must be chosen with extreme care. The external plume, however, will require a different treatment if accurate information is required outside of the dense core of the plasma blob. These conclusions are discussed more fully in Section 6 and recommendations for improvement of the thruster, additional experimentation, and further model development are presented there.

ii

TABLE OF CONTENTS

Accession For	
NTIS GRA&I	☒
DTIC TAB	☒
Unannounced	☐
Justification	
By	
Distribution/	
Availability Codes	
Dist	Avail and/or Special
A-1	

1. __INTRODUCTION__

The Teflon Pulsed Plasma Thruster (PPT) has been around for more than 15 years. Small (approximately one micropound thrust) versions have been proved feasible on satellites. Larger versions are currently being used, with one monitored for contamination on a satellite launched in the fall of 1982. The thruster of primary concern in this report is the much larger (one millipound thrust) model which is still in the process of being developed.

Since the principles of PPT operation are described in References 1 and 2, only a very brief outline is given here. A PPT consists of a pair of bar electrodes connected by a capacitor bank with external power supply, and a feed system which forces the Teflon "fuel" into position between the electrodes. This is shown schematically in Figure 1. The capacitor is charged between firings, as are the directly coupled electrodes. A minute amount of material is introduced into the electrode gap allowing an arc discharge. The high temperature arc across the face of the Teflon ablates, dissociates, and ionizes a small quantity of Teflon (producing a carbon-fluorine plasma) which supports the continuing discharge. The current flow induces a high magnetic field and reacts with that field to accelerate the plasma to velocities of several thousand meters per second, thus providing the thrust.

The very high exhaust velocity produces one of the PPT's most promising features, a specific impulse several times larger than that of chemical rockets. The exhaust itself poses problems, however. A serious concern of satellite designers is the exhaust plume's contamination potential. The plume of the PPT is known to contain primarily ionized carbon and fluorine, but additional small quantities of heavy molecules (metals and metal oxides stripped from the electrodes and insulators as well as fluorocarbons) probably exist. It is important to determine how much of what exhaust products may reach sensitive satellite surfaces.

The PPT's obvious potential for long life, dependable, accurate, and very efficient attitude control and station keeping functions, and its apparent potential as a contamination source have been the subjects of considerable

research. Reference 1 describes the work pertinent to the present study, and that material will not be reviewed in detail here, except to note that References 2 and 3 present attempts to model the internal and external plasma flow respectively. These models were adopted as the basis of this investigation, and will be discussed in some detail below. The internal model was developed for a thruster with an entirely different feed system and is inapplicable to the present device.

Important new experimental data available from investigations performed at the Jet Propulsion Laboratory and at the Arnold Engineering Development Center (Refs. 4, 5, and 6) have added to the data base which is a critical evaluation tool used to evaluate the models. This information and how it impacts various aspects of the model are discussed below.

2. THRUSTER OPERATION

Figure 1 shows the millipound thruster. The Teflon bars are forced against stops machined on the copper anode. The igniter is fired, releasing a minute quantity of ions and electrons into the space between the charged electrodes which then begin to discharge. The discharge initiates the ablation, dissociation and ionization of the face of the Teflon bars. The plasma thus formed supports the continuing current discharge which interacts with the induced magnetic field to accelerate the plasma.

The complete electrical circuit (consisting of capacitor bank, electrodes, and plasmoid, plus connections) behaves as a series R, L, C circuit. That is, the current exhibits damped sinusoidal variation as shown in Figure 2. The contribution of the plasma to the total circuit resistance and inductance should be variable since the amount of plasma in the interelectrode gap changes with time. (The contribution to the capacitance is negligible.) As shown in the figure, however, the data agree remarkably well with the simple damped sine wave obtained by assuming constant circuit inductance and resistance. The coefficients shown in the figure were determined by matching the data to the equation and these can be used to determine the circuit parameters (see Ref. 6).

2
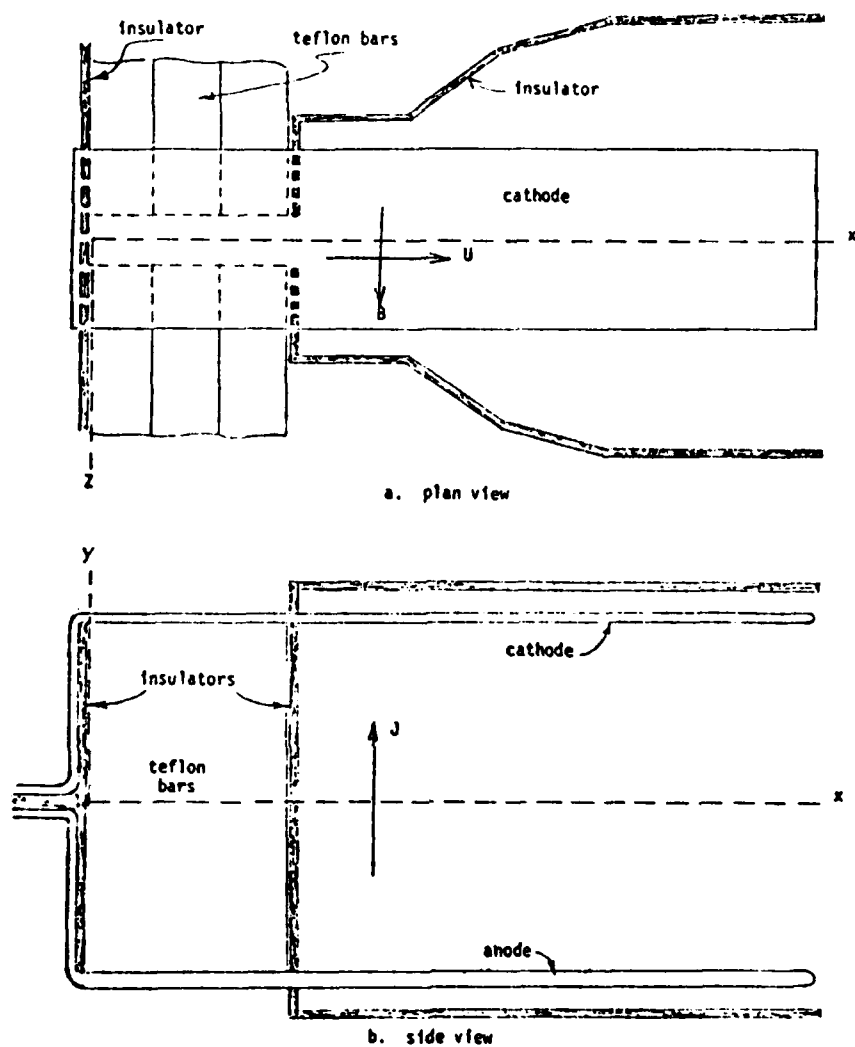
Figure 1. Scematic of Pulsed Plasma Thruster.

$C = 3.2(10^{-8})$ farad

$R = 1.3(10^{-2})$ ohm

$L = 9.7(10^{-8})$ Henry

It is possible that, at least during the first cycle (during which nearly all the plasma is formed), the plasma components of resistance and inductance are small compared to those of the fixed portion of the circuit, so that the totals are essentially constant. During the second current cycle very little

3

ENGINE DISCHARGE
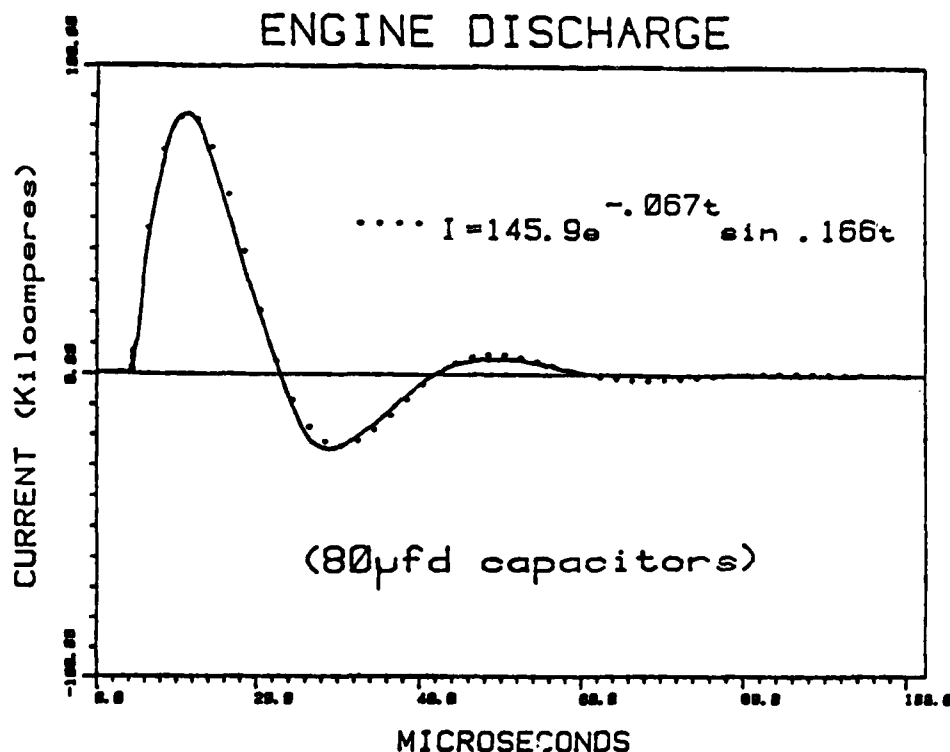
Figure 2. Circuit Current.

additional Teflon is ablated, and even less is ionized; thus the resistance is significantly increased and the damping is strongly enhanced. Similar data taken with smaller capacitors installed show this latter effect more strongly.

If one assumes that the amount of Teflon ablated per half-cycle of current discharge is proportional to the integral of the square of the current over that half-cycle (which is related to the energy consumed), one finds that some 92.1% is ablated during the first half-cycle, and 7.3% in the next half-cycle, leaving less than 1% for the remainder of the discharge. Such a drastic difference in plasma densities makes it unlikely that a single theoretical model can be developed to describe the entire process.

Further support for this assertion was sought by analyzing the (unpublished) data obtained by discharging the thruster through an aluminum shorting bar across the electrodes. This test was run in the atmosphere, and

4

the current history is again closely approximated by a damped sine wave. The parameters calculated for this circuit (with the shorting bar replacing the plasma) are

$$C = 3.2 \ (10^{-8}) \ \text{farad}$$
$$R = 1.4 \ (10^{-2}) \ \text{ohm}$$
$$L = 2.1 \ (10^{-7}) \ \text{Henry}$$

The fact that the resistance agrees well with that obtained from the plasma forming discharge strengthens the assertion that the resistance of the plasma is small. The significant (factor of two) increase in the inductance may be due primarily to the increase in the physical size of the current loop. (The shorting bar was located at the very end of the electrodes.)

The field vectors in Fig. 1 indicate the direction of the major field components during the first half-cycle of the discharge. It should be noted that the z-component of the magnetic field vector changes sign somewhere between the origin and the leading edge of the plasmoid. In the second half-cycle the J and B vectors reverse, but the acceleration vector does not. Reference 5 provides field data for the millipound thruster which appear to agree qualitatively with those for the micropound thruster given in Ref. 2. These data are discussed in Section 4.

3. MODEL DEVELOPMENT - OVERVIEW

A complete theoretical model of the PPT operation and plume can be partitioned into an internal model which would describe the circuit discharge, Teflon chemistry and plasma acceleration, and an external model which would describe the plume expansion beyond the ends of the electrodes. The internal model must realistically represent the physics of the plasma flow using appropriate field equations for the fluid flow parameters (densities, velocities, pressures, temperatures) and the electromagnetic field variables (electric field, magnetic field, current density, etc.). Also required are constitutive equations which describe the nature of the medium (transport coefficients, etc.) equations to model the formation of the plasmoid (ablation, ionization), and boundary conditions. The external model will also

5

The spectra exhibit sharp, well defined peaks characteristic of atomic rather than moleclar emission although fluorocarbons do emit in the 2300-3300 Å range (Ref. 6). This would seem to indicate that either the plasma environment is too severe for the heavy molecules to survive or that dissociation is complete.

The study also presents data obtained by monitoring the temporal history of several individual emission lines at the thruster exit plane. All of the lines monitored exhibit a strong pulse between 11 and 19 microseconds into the cycle and a second, much smaller (by as much as a factor of 10), pulse between 30 and 35 microseconds. The species so monitored include aluminum, neutral and ionized carbon, and fluorine. All pulses are quite similar in character and timing.

Several deductions about the nature of the plasma can be made from the above observations. The most important is that the flow is dominated by collision effects. That this must be the case is evidenced by the fact that atoms with vastly different (even zero) charge-to-mass ratios pass the exit plane at the same time, apparently with quite similar velocities. In addition, this information implies that, although the plasmoid is a highly complex mixture of species, a model which considers it to be a three, or even one, component fluid may be adequate to give reasonable accuracy.

A three component model might consist of neutrals, ions, and electrons, as suggested in Ref. 2. There it was proposed that an average molecular weight of 16.67 be used for the ions and neutrals (this being the weighted average for two fluorines to one carbon), and that the number densities of ions and electrons are equal (assuming charge neutrality and single ionization).

In this author's opinion, we know both too much and too little to adopt this model. First, it is apparent that single ionization is not a good assumption. Also, it is quite likely that the average molecular weights of the ion gas and the neutral gas are not equal since the ionization potentials of carbon and fluorine are quite different. On the other hand, sufficient data are unavailable to enable one to predict with any confidence the energy

transfer between the various gas components. Reference 2 presents much pertinent data, such as dissociation and ionization energies, as well as a model for ionization rates. Of importance here is the fact that the total energy required to ablate, dissociate and ionize the total mass of Teflon is a small fraction of that available or required to accelerate the plasma to such high velocities. Since reaction rates, collision cross sections, etc., are unknown, it seems inappropriate to include such refinements in a model at this time. In fact, no data are available with which to compare the output of such a model. It would seem preferable, as well as much simpler, to model the plasma as a single conducting gas. In this case, the conservation equations consist of one mass equations, one to three momentum equations (depending on dimensionality of the model), and one energy equation.

Of course, there are inaccuracies built-in to such a one fluid model. For example, doppler shift spectroscopy measurements (Ref. 7) seem to indicate somewhat different velocities for different species. These data, however, are not entirely consistent and are difficult to interpret. Another anomaly is demonstrated by the data taken at different positions relative to the thruster axis (Ref. 5). These show considerable variation in the intensity of certain emission lines with position. Again, interpretation is difficult.

Some approximate calculations have been performed to check the validity of the above assertions. The mean free path in the plasma is essentially proportional to the inverse of the number density, n, whereas the Debye length is proportional to the square root of temperature/number density. Total collision cross sections of carbon and or fluorine atoms are unavailable, but assumed diameters on the order of 10^{-10} m give a mean free path λ of about $10^{19}/n$ m. The Debye length is given by

$$\lambda_D = (\varepsilon_o KT/n_i e^2)^{\frac{1}{2}} \tag{1}$$

where $_o$ is the free space permitivity, k is Boltzman's constant, T is temperature, n is the ion number density and e is the electron charge. This formula yields

$$\lambda_D = 69(T/n)^{\frac{1}{2}} \text{ meters with T in Kelvin.} \tag{2}$$

To approximate the number density in the plasmoid one can refer to photographic evidence. At 11 sec after initiation the plasmoid just about fills the interelectrode volume, and about half of the first half-cycle energy has been deposited. Assume, then, that about .7 mg of material with an average molecular weight of 16.67 occupies a volume of $1.5(10^{-4})$ m^3, for the number density of the first plasmoid. These approximations then yield a mean free path λ of $5(10^{-5})$ m. The additional assumptions that the plasmoid is about 20% ionized yields a Debye length λ_D of $8(10^{-8})$ m. The first figure allows the use of continuum equations as is small compared to physical dimensions, and since $\lambda_D \ll \lambda$ the assumption of charge neutrality is also valid.

It must be noted, however, that the above computations are valid only for the first plasmoid (that produced by the first half-cycle of the discharge). As the ablated mass appears to decrease by an order of magnitude with each successive half-cycle, the mean free path will increase accordingly, and certainly by the third half-cycle the continuum hypothesis breaks down. The Debye length also increases, but inversely as the root of the density. Thus a model developed to describe the first plasmoid may not be accurate for the second one, and certainly will not apply to any subsequent emissions. Unfortunately, from the viewpoint of contamination analysis, it may be that the latter portion of the thruster exhaust is of prominent importance.

For the reasons given above, it is suggested that the one fluid model be developed further. For such a model the governing equations represent conservation of mass, energy, and three components of momentum, coupled with Maxwell's equations of electromagnetics. These can be written as:

$$\rho_t + div\ (\rho\ \underline{v}) = 0 \tag{3}$$

$$e_t + \underline{v} \cdot grad \quad = conduction + dissipation\ effects \tag{4}$$

$$\rho\underline{v}^t + \rho\underline{v} \cdot grad\ \rho = Lorentz\ body\ force + viscous\ forces \tag{5}$$

$$div\ \underline{E} = 0 \tag{6}$$

Curl $\underline{E} = -\underline{B}_t$ (7)

div $\underline{B} = 0$ (8)

curl $\underline{B} = \mu(\underline{J} - \epsilon_o \underline{E}_t)$ (9)

Here ρ = gas density,

$\underline{v}$ = gas mean velocity,

t = time, and $(\rho)_t$ represents partial differentiation w.r.t.t,

e = energy per unit mass,

p = gas pressure,

$\underline{E}$ = electric field intensity,

$\underline{B}$ = magnetic flux density,

$\underline{J}$ = current density,

μ = magnetic permeability, and

ϵ_o = vacuum permittivity.

To these equations must be coupled constitutive equations which further describe the medium itself.

4.2 Constitutive Equations

The most general, one fluid plasma models with strong magnetic fields present the constitutive equations as tensor relationships. That is, such plasmas are nonisotropic, with the direction of the magnetic flux density vector $\underline{B}$ being a "preferred direction" in the sense that material properties in this direction differ from those in perpendicular directions. The

10

properties involved include both electric and thermal conductivities and the viscosity. These control the right-hand sides of the momentum and energy equations above, and therefore, some preliminary analysis is in order at this time.

Any computation of plasma transport coefficients is an estimate. Since no experimental data exist for a plasma resembling that produced by the PPT, one is required to make such an estimate. Reference 8 presents a theory for computing transport coefficients for a two component plasma (singly charged ions and electrons). In particular, this theory allows one to estimate the different components of the transport tensors.

The strength of the magnetic field is conveniently described by the cyclotron frequency for the ions

$$\Omega_i = eB/m_i \qquad\qquad (10)$$

where e is the ionic charge and m_i, the mass. This is the frequency at which a single free ion would orbit. For a singly charged ion of atomic mass number 16.67 (mass = $2.88(10^{-26})$ kg) and a field of about .5 Telsa (which is appropriate for the first plasmoid),

$$\Omega_i = 3 \ (10^6) \ sec^{-1}. \qquad\qquad (11)$$

A measure of the collision effect is a collision time which can be estimated from

$$\tau_i = \frac{40 \ \pi \ \epsilon_o \ m_i^{\frac{1}{2}} \ (KT)^{3/2}}{n_i \ e^4 \ \log \Lambda} \qquad\qquad (12)$$

where $\Lambda = 1.24 \ (10^7) \ T^{3/2} \ n^{-\frac{1}{2}}$.

For a temperature of 40,000K and a number density of 10^{23}, the above equation yields a collision time of about 10^{-9} sec. Since the orbital frequency $\Omega_i = 3(10^6) \ sec^{-1}$, it is apparent that an ion would experience many collisions per orbit. This calculation substantiates the assertion that the process is

11

collision dominated, and also implies that a scalar approximation for the transport coefficients is appropriate. Since the collisions are randomizing events, the "preference" for the direction parallel to the magnetic field is lost. When an ion begins to react to the presence of the field, it suffers a collision and is redirected.

It still remains to provide some model for the magnitudes of the scalar transport coefficients. Theoretical estimates based on kinetic theory are available, but all such theories presume plasmas of a much less complex composition than the one produced by the PPT. Thus any model chosen will impart a serious uncertainty concerning the calculations, unless the coefficeints are of such magnitude that variations do not alter the flow in a significant fashion. Otherwise, experimental model verification will be needed.

Reference 8 provides some formulae for transport coefficients, based on a two-component plasma (i.e., highly ionized), as follows:

$$\sigma = .74 \ \frac{ne^2 \ \tau_e}{M_e} \qquad \text{= electrical conductivity} \qquad (13)$$

$$\kappa = 2.9 \ \frac{nKT \ \tau_e}{Me} \qquad \text{= thermal conductivity} \qquad (14)$$

$$\eta = .5 \ nKT \ \tau_i \qquad \text{= viscosity} \qquad (15)$$

where τ_e is the collision time for the electrons and is equal to $(Me/M_i)^{1/2} \ \tau_i$. Using these formulae with numerical values appropriate to the first plasmoid yields the following order of magnitude estimates

$$\sigma = 10^4 \ \text{mhos/m,} \qquad (16)$$

$$\kappa = 10 \ \text{J/sec K, and} \qquad (17)$$

$$\eta = 10^{-8} \ \text{N·S/m}^2, \qquad (18)$$

To examine the validity of these estimates, one must rely on some very rough comparisons with available data. For example, in the case of conductivity, if it is assumed that the plasmoid provides a 20 cm^2 cross section for current flow between the electrodes which are about 8 cm apart, the above conductivity yields a total resistance of about $4(10^{-3})$ Ω. This is about one-fourth of the total circuit resistance as determined by the current discharge measurements (see Section 2) which is probably high, but not completely unreasonable according to the earlier assertion that the plasma resistance is small.

The viscosity above with appropriate values of velocity (10,000 m/s) and density (3×10^{-3}kg/m^2) gives a Reynolds number

$$Re = 10^8 \tag{19}$$

which implies that viscous forces are negligible except within an extremely thin boundary layer along the electrodes. It is thus proposed to ignore viscous terms in the model. The only experimental verification of this assumption is that plasmoid photographs seem to indicate fairly uniform velocity profiles which would not occur under the action of strong viscous effects.

With nothing better than a rough global estimate of temperature, no similar conclusions may be drawn concerning heat transfer. In fact, considering the intensity of both the UV emission and visible emission from the plasmoid; it is possible that radiation is more important in heat transfer than thermal conduction.

At this point the choice of transport coefficient models is not entirely clear. A reasonable approach would seem to be to use the above expressions for electrical and thermal conductivity and to ignore viscous effects. (Note that, unlike ordinary gases, plasmas conduct heat primarily through the electrons and therefore thermal conduction and viscous diffusion are not coupled by a Prandtl number near unity.)

13

One further simplification of the model equations is usually made in magnetohydrodynamic theory, namely the neglect of the displacement current, $\varepsilon_o \underline{E}_t$, compared with the conduction current $\underline{J}$. The magnitudes of the variables in the first PPT plasmoid are compatible with this simplification (which is quite significant), but some caution is required. In the vacuum ahead of and behind the plasmoid there can be no conduction current. The electric and magnetic fields, however, do not vanish (or become uniform). Disturbances propagate with the velocity of light, which is much higher than either the ion velocity or the Afvèn wave propagation in the plasma. Thus, the MHD equations can be used within the plasmoid, but the computation domain must contain only that region in space so occupied. The boundaries of the computation domain thus move and must be relocated at each time step. The boundary conditions applied at these boundaries match the field variables across the plasmoid/vacuum interface.

Applying the simplifications above to the general equations, eliminating the electric field using the generalized Ohm's Law with scalar conductivity,

$$\underline{E} = \underline{B} \times \underline{V} + \underline{J}/\sigma \tag{20}$$

and eliminating the current density using

$$\underline{J} = \frac{1}{\mu} \text{ curl } \underline{B} \tag{21}$$

(which is a result of neglecting displacement current) produces a familiar set of equations

$$\rho_t + \text{div}(\rho \underline{V}) = 0 \text{ and} \tag{22}$$

$$\rho u_t + \rho \underline{V} \cdot \underline{V} + \text{grad } p = \sigma(\underline{E} + \underline{V} \times \underline{B}) \times \underline{B}. \tag{23}$$

To these must be added the algebraic equations of state

$$p = \rho RT, \tag{24}$$

$$e = c_p T \tag{25}$$

14

and either the above expressions for   and   or some other model. The state
equations here assume a perfect gas.   Assuming a monatomic gas with atomic
weight 16.67 gives R = 500 c_p = 2.5R.   (26)

4.3 One Dimensional Model

This model should reasonably approximate reality. For the purpose of the
present study, the model was further simplified for numerical implementation.
First, the dimensionality of the model was reduced to one by neglecting
variations in the y and z directions and by considering only the x-component
of $\underline{V}$, the y-component of $\underline{J}$, and the z-component of $\underline{B}$. It is apparent that,
while these are indeed the dominant components of thee vectors, the one
dimensional model can provide only a general description of the process.
Because of this limitation and the uncertainty in the transport coefficients
η and κ the dissipation (Joule heating) and heat conduction terms were
dropped and temperature was assumed to be constant.   The one-dimensional,
isothermal model is governed by the equations

$$\rho_t + (\rho u)x = S,$$ (27)

$$(\rho u)_t + px = \frac{1}{\mu} BB_x,$$ (28)

$$B_t + (uB)_x = 0, \text{ and}$$ (29)

$$p = \rho RT \quad (T \text{ constant}).$$ (30)

Here the source term S must be introduced since the addition of plasma
due to the ablation and ionization of Teflon occurs over the first few
centimeters in the x-direction.   In the full three-dimensional model this
material addition would appear as a boundary condition.

The source function is one of the weakest points in model development
(whether here or as a boundary condition). The rate of Teflon ablation must
depend on the energy flux at the surface. Unfortunately, energy transfer in
the plasma is not well understood.   Conductivity models have not been
experimentally verified, temperatures have not been measured, and radiation in

15

the IR range has not been measured. In addition, ablation rates are known only at much lower temperatures. Thus, the ablation model is very uncertain. For the purpose of testing the one-dimensional isothermal model, it was assumed that the source term in the mass conservation equation is proportional to the square of the current density at a particular value of x, as long as x < 4.5 cm (the extent of the Teflon surface). Even here the proportionality factor is a matter of conjecture and numerical experimentation.

Coupling the ablation rate to the total current flow at any time (as proposed in Ref. 2) is inappropriate, especially for the side feed thruster currently under consideration. The ablation is a much more localized phenomenon as the Teflon fuel cannot "see" the bulk of the plasma. Thus, even if radiation is the primary heat transfer mechanism, only that plasma located in the narrow "combustion chamber" between the Teflon bars can contribute. After a few microseconds, the bulk of the current flow is well out between the electrodes. In fact, according to the current flow data of Ref. 5, the current flow extends well past the electrodes as the plasmoid emerges from the thruster.

The ablation model suggested here effectively assumes that ablation, dissociation, heating, and ionization times are short enough to be neglected, and that the actual power source which accomplishes this is that produced by the current flow. In a two-dimensional flow model a similar device could be used (assuming uniformity in the z direction), but in a full three-dimensional model ablation would take place on a boundary surface. In the latter case additional investigation into exactly what portion of the plasma contributes to the local heat transfer would be required.

A drastically simplified set of equations has been proposed to describe both the plasma motion and the magnetic field. One consequence of the simplifications made can be examined without recourse to numerical implementation of the model (which is impossible without a set of initial and boundary conditions). The neglect of the displacement current reduces Faraday's equation to

$$\frac{1}{\mu}\operatorname{curl} \underline{B} = \underline{J} \tag{31}$$

as discussed above, and allows the elimination of $\underline{J}$ from the equations. The reduction of the system to the one-dimensional model produces

$$J = - \frac{1}{\mu} B_x \qquad (32)$$

where J and B are the y and z components respectively. In fact, although symmetry through the z=0 plane implies that B_1 (the x-component of $\underline{B}$) is zero, it cannot be true that $B_{1z} = 0$ unless the medium is unbounded in the z-direction (as the one-dimensional model implies). Comparison of current flow and magnetic field data indicates that current density is not proportional to the magnetic field gradient along the axis as the model implies. This could be the result of failure of the one-dimensional simplification, or could result from the fact that the probes used to measure the current and field disturbed the flow. It is not believed that the displacement current could be responsible.

4.4 Boundary and Initial Conditions

The boundary conditions and the correct handling of them in the numerical implementation of any fluid mechanical model are crucial to the success of the effort. Accuracy of the solution near the boundaries is obviously affected, but, in some cases, changes in boundary conditions will actually prevent the numerical algorithm from working. This seems to be the case with the present model, and the results are not those anticipated at the onset of the project. This section is a discussion of the boundary conditions for the one-dimensional isothermal model, as well as for the more general model developed above. Many of the difficulties appear in even the simple case.

4.4.1 The Simple Model - At the x=0 end of the interelectrode gap the region is bounded by an insulating plate which protects the electrical circuitry from the plasma. This solid wall requires the velocity u to vanish at x=0. The condition on the magnetic field is more difficult to assess. Beyond the insulator the electrodes are bent and brought together (but for a thin insulator) and beyond that the electrical connections to the capacitor bank are made. Thus, a conducting plate carries a very large current in the y-direction just a few millimeters in the negative x-direction from x=0. This

current, as well as the current flow through the plasma (in the positive x-region), induces the magnetic field near x=0. A simple calculation of the magnetic field induced by a sheet current (assuming quasistatic conditions, since the current variations are slow compared to the speed of light) predicts a magnetic field directly proportional to the total current (as expected). Adding the effect of a volumetric current flow to represent (in a crude way) the plasmoid current maintains the proportionality changing only the coefficient. As previously discussed, the total circuit current varies as a damped sine wave. Reference 6 shows the magnetic field variation as obtained experimentally. No explanation is suggested for the deviation at the early times, but, in general, the correlation with a damped sine wave is excellent. Numerical values for the geometry of the thruster were used in a calculation to predict the proportionality constant for the relation

$$B(o,t) = CI_{tot}(t) \qquad\qquad (33)$$

and this was compared with the experimentally obtained value. It is felt that the agreement (within 20%) is very reasonable, considering the approximations made.

Thus, if the circuit current as a function of time is known, the magnetic field at x=0 is also known, and this provides a necessary boundary condition for the model. In light of the discussion in Section 2, it may be that the necessary current trace can be obtained from the circuit parameters, without being dependent on the plasma flow. If so, this boundary condition on B represents the only coupling between the plasma flow and the external circuitry. Otherwise some global condition coupling the total plasma current, resistance, and inductance with the external circuit parameters must be applied at each time step.

The conditions on u and B at x=0 are sufficient for that boundary. No condition can be applied to ρ . The line x=0 in the x, t-plane is a streamline (dx/dt=u=0) and is a characteristic of the equations, which provides the correct variation of density there.

18

The necessary conditions for the moving boundary at the leading edge of the plasmoid are more difficult to obtain. The first decision to be made is the manner in which the boundary is to be defined. This must be done so that the equations of the model are valid inside the boundary and so that the vacuum equations are valid (at least to a reasonable approximation) outside the boundary.

Near the leading edge of the plasmoid, at least during the early part of the discharge, the magnetic field is in the negative z-direction while the current is in the positive y-direction. The Lorentz force is thus in the negative x-direction and this should tend to sharpen the boundary. That is, any very low density plasma will be slowed until the denser plasma (with the higher pressure) catches up, and collisions once again dominate the acceleration process. Thus the description of the leading edge as a sharp boundary seems reasonable. This argument is further enhanced by examination of the time resolved exit plane spectroscopic data of Ref. 6. A possible means of defining this boundary is to advance it in the x-direction with the velocity of the plasma at that location and time, as determined by the plasma equations. The region ahead of the front is thus assumed to be a vacuum in which the static form of the electromagnetic field equations apply (since the speed of wave propagation is so much larger than the front velocity). The density is then determined from the fact that no plasma crosses the advancing front, and a boundary condition on the magnetic field can be obtained by comparing the mass and field equations along the line dx/dt = u (neglecting the source term at the front, which is appropriate at least for x > 4.5 cm).

The mass equation can be rewritten

$$\frac{D\rho}{Dt} + u_x = 0 \tag{34}$$

and the field equation

$$\frac{DB}{Dt} + BU_x = 0 \tag{35}$$

19

usual material derivative. Combining

$$(36)$$

$$(37)$$

$$(38)$$

re is an inconsistency in the one-
$- \frac{1}{\mu} B_x$ approximation mentioned above.
and $B(x_0, t)$ can be calculated from

$$(39)$$

it depth (z-direction). This equation
or $B(x_0)$ since $B(o)$ has already been
predicts that $B(x_0)$ should behave like
the data. Again it is felt that the
nsional model.

th initial conditions. The initiation
with electron flow from the igniter
ediately attaches to the main cathode
ted telfon. To describe this process
re a moving boundary at the back as
so a later time in the process was
Initial conditions compatible with the
ter initiation of current flow were

4.4.2   The General Model
general three-dimensional model is
reasoning. The boundaries of the
thruster at x=0, the electrodes at
$x \leq L$, the plasma-vacuum interfac
sides $z=\pm z_0(x,y,t)$, for $x > L$.

Even in the general model it
certain of the field components.
available data. For example; phot
any, expansion in the z-direction.
Lorentz force is directed inward a
force and containing the plasmoid.
be neglected in even the general n
described adequately by $z=\pm w/2$ whe
between the Teflon faces in the
evidence, however, that the plasmo
cathode than at the anode. No exp
front appears to be quite flat in t
function of y and t only.

At the insulator at x=0 the
taken proportional to total curre
function of y. The x-component
boundary (due to the proximity of
and the y-component can probably be

The electrode surfaces at $y=\pm h$
and the y-components of velocity
insulators and have no effect on th
a new model is needed for the abl
produced at these boundaries.

Thermal boundary conditions,
somewhat arbitary at this time. At
the PPT, it has been found that a
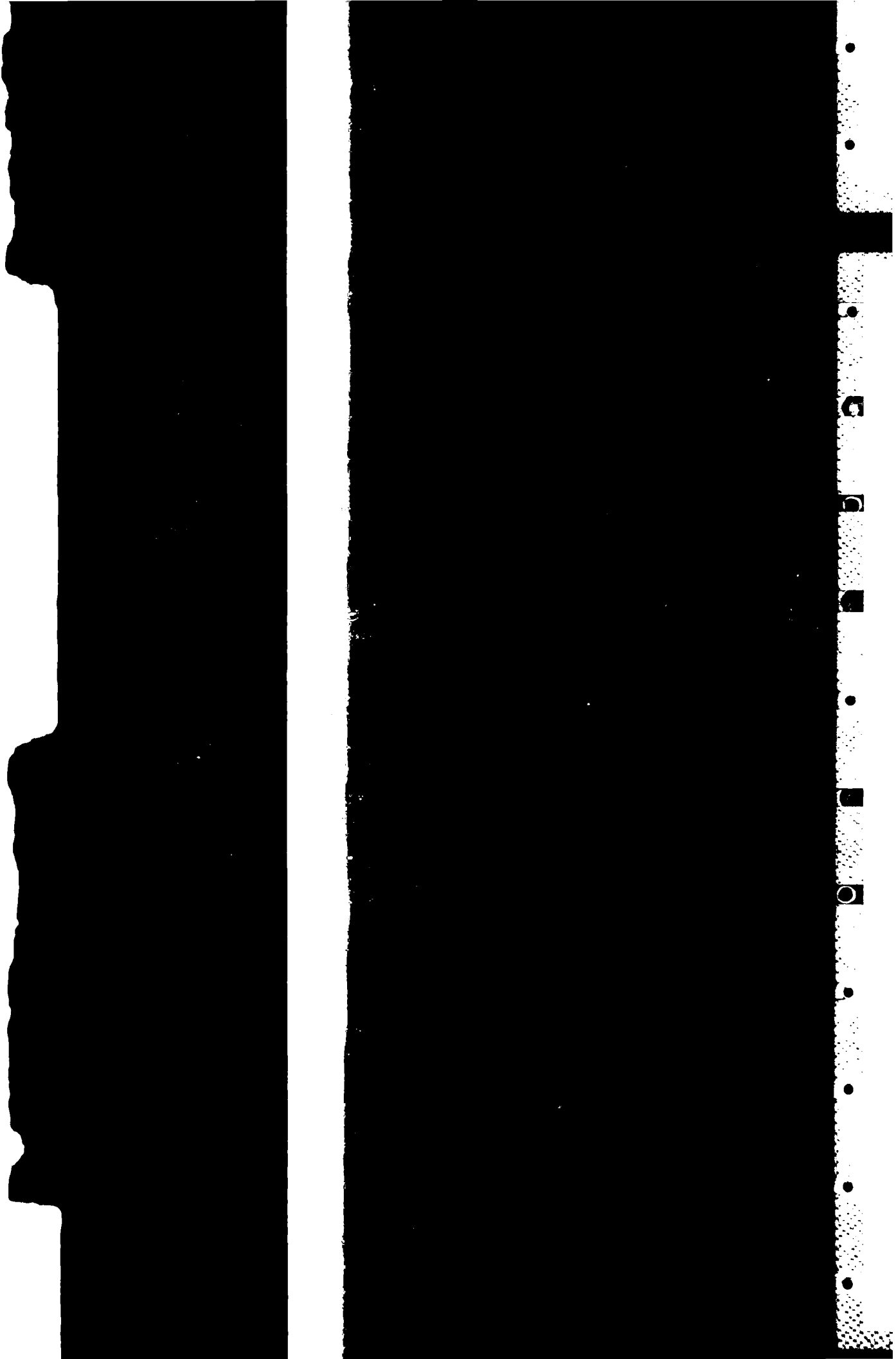
640°C independent of gas temperature, and this may be used as the boundary condition. A constant temperature condition may also be appropriate at the electrode surface. While there is very little copper appearing in the plasma, a temperature near the melting point may be assumed. On the other hand, the insulator at $x=0$ seems to adequately protect the circuitry from the plasma suggesting a zero heat flux condition.

As can be deduced from the discussion above, there is some guess work involved in selection of proper boundary conditions. This uncertainty, added to those mentioned in Section 4.2 concerning the basic equations and transport coefficients, reduces the probability of obtaining a realistic description of the acceleration process using such a model. It was decided not to construct a numerical algorithm to experiment with any more than the drastically simplified one-dimensional isothermal model, and even that proved to be very dependent on unjustifiable assumptions.

4.5 <u>Numerical Model</u> - An explicit, forward time step, finite difference algorithm was chosen to numerically test the simple model developed above. Although a characteristic method or an implicit finite difference method might be more appropriate for the simple model, these would be very difficult to generalize to the multidimensional dissipative model. The specific algorithm chosen was a Lax-Wendroff type, similar to that presented in Ref. 2. The equations are written in conservative form

$$w_t + f_x = 0 \tag{40}$$

where w is a component of the variables vector (ρ, ρu, B) and the f components are functions of the variables. A single time step is taken in two parts, and central differences are used for the x-derivatives. Thus, if $w_{n+\frac{1}{2}}^{j+\frac{1}{2}}$ represents the variable w at the nth grid space and jth time step, the equations can be written:

$$w_{n+\frac{1}{2}}^{j+\frac{1}{2}} = \tfrac{1}{2}(W_{n+1}^{j} + W_n^{j}) - \frac{\Delta t}{2x}(f_{n+1}^{j} - f_n^{j}), \tag{41}$$

$$f_{n+\frac{1}{2}}^{j+\frac{1}{2}} = f\left(w_{n+\frac{1}{2}}^{j+\frac{1}{2}}\right) \quad \text{and} \tag{42}$$

22

$$w_n^{j+1} = w_n^j - \frac{\Delta t}{x}(f_{n+\frac{1}{2}}^{j+\frac{1}{2}} - f_{n-\frac{1}{2}}^{j+\frac{1}{2}}) . \tag{43}$$

This procedure must be modified for the density equation to include the source term in which B_x is replaced by a central difference.

Schemes such as this are known to be numerically unstable if the time step is longer than the time required for information to propagate over one grid space. Thus the local sound speeds and Alfvén wave speeds must be computed at each time step, and the next t chosen accordingly. Here t was taken to be

$$\Delta t = \frac{x}{< \left|u_n^j\right| + \left[RT + B_n^{j2}/\mu\rho \quad _n^j\right]^{\frac{1}{2}}} \tag{44}$$

The boundary conditions on B and u at $x=o$ are applied directly. The boundary values for ρ are computed by applying the continuity condition to a one-sided grid space (allowing no mass to cross the boundary). The same technique is used for ρ at the moving boundary $x = x_o(t)$, but only after that boundary is located.

The moving boundary is first located according to $x_o^{j+1} = x_o^j + u_n^j \Delta t^j$. Then Δu is computed as the average of the predicted values at j and $j + 1$ from

$$u_t = -\frac{BB_x}{\rho^u} + \frac{RT\rho_x}{\rho} . \tag{45}$$

The boundary is relocated using the new average velocity, and the procedure is repeated until the new position of the boundary converges. Only then can the new boundary values of ρ and B be computed.

At this point in the procedure, the last grid space is generally larger than the others due to the shifting of the boundary point. Before restarting the next time step, the grid points are respaced evenly over the range $o \leq x \leq x_o$ and the corresponding variable values are determined by quadratic interpolation.

Several test runs were performed using the computer code the model described. In these runs, the coefficients of the source function in the density equation, the coefficient in the boundary condition for $B(o, t)$, and the initial conditions for $p(x, o)$ and $u(x, o)$ were varied. The initial conditions for $B(o, t)$ were taken to match the field data from Ref. 6 at five microseconds; i.e., a linear variation from $B(0)$ with negative slope. The results depend strongly on the initial conditions and parameters chosen, and most choices seem to produce an instability which is triggered by very steep gradients at the plasmoid front $(x = x_o)$ and which propagates back into the solution domain. These instabilities are unlike those reported in Ref. 2, as they are not caused by high Alfven wave speeds or by a violation of the stability criterion above.

The problem appears to be caused by the fact that, with the initial conditions assumed, the Lorentz force in the negative x-direction at the front is larger than the pressure force in the positive x-direction, and the front decelerates. This may be strictly a product of the mathematical modeling and/or the numerics. On the other hand, the physics of the thruster may be such that the discharge is actually like a detonation as opposed to a deflagration, and a shock type structure exists near the front. The present model has no capability of "capturing" or "fitting" such a discontinuity and will indeed be unstable in this case. The time resolved spectroscopic data of Ref. 6 do not seem to indicate a shock as the plasmoid exits the thruster since the leading and trailing edges exhibit a similar sharpness.

The question remains unresolved at this time, and recommendations for further research follow.

5.   MODEL DEVELOPMENT-EXTERNAL

5.1 Monte Carlo Simulation

Far less progress has been made on a model of the external plume. The first plasmoid of thruster exhaust is quite definitely a continuum as it passes the exit plane. This can be seen from photographic evidence which shows a distinct shock wave produced as the plasmoid flows over a probe in the

24

axis, as well as from estimates of the density made from the exit plane data of Ref. 6. Furthermore, the shock angle in the photographs is consistent with temperature estimates and observed plasma velocity. The central core of the plasmoid apparently remains dense enough to behave as a continuum for quite some distance, eventually expanding into the surrounding vacuum.

The outer regions of the plasmoid, however, pass quickly from the continuum to the rarefied regime, probably immediately after exiting the thruster. At this point, the only modeling technique which appears promising is the Monte Carlo technique. The simulation of the flow using Monte Carlo methods can, in principle, properly model the transition from continuum to rarefied to free molecular flow as the edges of the plume expand outward.

Monte Carlo methods predict the flow from statistical analysis of the particle collision processes, and have been demonstrated to produce very acceptable results when properly applied. Unfortunately, many of the data required to properly begin the Monte Carlo analysis are not yet available. We have a reasonable amount of information about the constituents of the exit plane exhaust. The complexity of the exhaust is somewhat disheartening, however. Mention has been made of the many types of ions and neutrals detected, including multiple ionized carbon and fluorine, as well as traces of various metal ions. The variety of possible interactions is very large, and it is not obvious how many of the possibilities must actually be accounted for in the model. It is unlikely that the one ion-one neutral model of Ref. 3 will be sufficient to accurately describe the situation.

After characterizing exit plane flow, it is necessary to provide the model with cross sections for the various types of possible collisions, and these cross sections are not readily available.

In addition, there is some evidence that some ion-electron recombination and neutralization take place within a meter of the exit plane. This is at least one possible explanation of the plume's change in color from blue-white to red as it progresses downstream. Flourine ions emit at several visible wavelengths, whereas neutral fluorine emissions are concentrated in the red range.

25

To further complicate the modeling problem, as the plasma expands and the density decreases, the point will be reached when collisions no longer dominate the process. It has been determined that, while some recombination probably occurs, significant quantities of ions persist, even through wall collisions in testing chambers. The ion and electron motion induces magnetic as well as electric fields, and electromagnetic forces will eventually dominate the flow as collisions become less frequent. Thus an accurate model would have to account for the long range magnetic field forces as well as the short range particle interactions.

Because of the difficulties and uncertainties expressed above, although Monte Carlo simulation of the PPT plume would undoubtedly provide some interesting and useful analysis, at this time it is doubtful that a definitive plume model can be developed with sufficient reliability to predict satellite contamination potential. Before potential users would have confidence in the model, more experimental verification would be necessary. Some of the presently available experimental data are discussed in the next section.

5.2 Experimental Problems

Although considerable effort has been expended in attempting to characterize the PPT plume, the extremely energetic nature of the plasmoid has made most plume data suspect. It is known that the fastest particles in the first plasmoid travel at about 40,000 m/s. These particles can rebound from the walls of a typical testing chamber and reenter the plume participating in spurious collisions, altering the flow pattern. This contamination of the plume is further augmented by electrons freed from the chamber walls (and other objects within the chamber) by the intense UV emission from the thruster, and by material sputter eroded from the walls by the fast ions.

The difficulty of separating direct discharge effects from chamber effects was a primary reason for altering the study plan of Ref. 6 to concentrate on the internal and exit plane flow; the other reason being the basic need for this type of data in its own right.

6. RECOMMENDATIONS FOR FURTHER RESEARCH

Much additional experimental and numerical research is required before a truly reliable computer code can be developed. The nature of much of the required work is apparent. This section presents the author's opinions and suggestions concerning possible research projects.

6.1 Internal Flow

The one fluid internal model should be quite adequate, once the boundary and initial conditions are properly confirmed, to model internal flow. A more complete mapping of current, magnetic field, and temperature between, and just beyond, the electrodes is required. One conclusion of this research is that the one-dimensional model tested is too restrictive to reasonably predict field patterns. No data exist for comparison of off-axis predictions from a multidimensional model. This comparison is mandatory if the multidimensional code is to be considered reliable, due to uncertainties in the theory.

Probably the most serious understanding gap concerns the ablation process itself. At this time the selection of a means of coupling the ablation rate to the various flow parameters, such as field intensity and temperature, is mostly guesswork. It seems reasonable to assume that the rate is somehow related to the energy of the "adjacent" portion of the plasma. Here "adjacent" must be defined in terms of grid spaces in the numerical model, and the number of spaces to be included depends on the radiative energy transfer. The intense radiation would indicate a relatively great amount but the clean white Teflon surface is a poor radiation absorber. It is for the purpose of increasing understanding of the energy transfer that temperature, as well as field data, is desirable. The means of acquiring these temperatures is not apparent.

Examination of the Teflon bars after many PPT firings reveals an area of excessive ablation from a region one to two centimeters from the anode. This suggests a "hot spot" in the region of the plasma. Many additional pulses produce no additional change in the bar surface shape. That is, the steady-

27

state shape has been reached, with the Teflon surface recessed in the region of the "hot spot". This is another indication of the one-dimensional model's inadequacy.

Once the data suggested above are available, computer experimentation with the multidimensional model can proceed.

6.2 External Plume

A complete model for the external plume is still further off. Here there are even greater uncertainties, as mentioned in section 5.2, and much additional experimentation is required. Any attempt to map the PPT's external plume must be executed with utmost care and planning. Particle collection must be made on a time-of-flight basis, and the particle velocity, mass, and charge must all be measured. The combination of velocity and time data will allow the researcher to distinguish between direct exhaust particles and those which have made one or more wall collisions before entering the collection device. The necessary complexity and precision required of such a project will make it a high-risk and expensive program, but it appears to be the only possibility of obtaining reliable plume data.

Even an extensive research program of this type will not be conclusive in the backflow region, which is so crucial to the contamination question. There it is insufficient to merely use speed and time of arrival to characterize a particle. It is likely that a significant portion of the particles reaching the backflow region are particles backscattered from the plume. In a chamber, this process is interferred with by particles scattered from the walls so this portion of the backflow cannot be measured with any real degree of reliability. Thus, while that portion of the backflow which comes directly from the engine can perhaps be distinguished using the methods described above, the remaining backflow from the plume cannot be so distinguished as the chamber effects cannot be accounted for.

This leaves space experiments as the final measurement of backflow and thus contamination potential. Such tests are extremely expensive and produce very few data points-per-dollar. They are, however, the tests which will be most acceptable to satellite designers, the potential users of the PPT.

REFERENCES

1. Yannitell, D. W., Pulsed Plasma Plume Modeling Study, SCEEE Summer Faculty Research Program, Final Report, 1980.

2. Palumbo, D. J., and Begin, M., Plasma Acceleration in Pulsed Ablative Arc Discharges, AFOSR-TR-77-0623, April 1977.

3. Palumbo, D. J., and Begin, M., Experimental and Theorectical Analysis of Pulsed Plasma Exhaust Plumes, AFOSR-TR-78-1242, 1978.

4. Plessa, L. C., Rudolph, L. R., and Fitzgerald, D. J., Plume Characterization of a One-Millipound Solid Teflon Pulsed Plasma Thruster - Phase I, AFRPL-TR-78-63, 1978.

5. Plessa, L. C. Rudolph, L. K., and Fitzgerald, D. J., Plume Characterization of a One-Millipound Teflon Pulsed Plasma Thruster - Phase II, AFRPL-TR-79-60, 1979.

6. Dawbarn, R., McGuire, R. L. Steely, S. L., and Pipes, J. G., Operating Characteristics of an Ablative Pulsed Plasma Engine, AFRPL-TR-82-017, 1982.

7. Thomasson, K. I., and Vondra R. J., "Exhaust Velocity Studies of a Solid Teflon Pulsed Plasma Thruster," J. Spacecraft and Rockets, Vol. 9, No. 1, January 1972.

8. Clemmow, P. C., and Dougherty, J. P., Electro Dynamics of Particles and Plasmas, Addison Wesley, New York, N. Y., 1969.

END

FILMED

8-85

DTIC